



Pairwise control in swarm flocking with application to UAVs

Jintao Liu^a, Ming He^{a,*}, Peng Xu^a, Xiangyang Deng^b

^a Command and control engineering college, People's Liberation Army Engineering University, Nanjing, 210007, China

^b Naval Aeronautical University, Yantai, 264001, China

ARTICLE INFO

Keywords:

UAVs swarm
Pairwise control
Sliding mode
Flocking
Distributed control

ABSTRACT

We propose a pairwise cooperative mode and control method to perform short-range cooperative missions of two specific UAVs in a swarm. The pair of UAVs can converge simultaneously to a specified distance and keep flocking with others. For pairwise control, we propose a new sliding mode control architecture including “Quadratic Error Sliding Surface” and “Sliding Mode Sign Multiplier”, which have the advantages of simple parameter design, high precision, and anti-disturbance ability. The proposed sliding surface is reachable, and the controller is stability which is proved based on the Lyapunov stability theory. Finally, to verify the influence of the pairwise control effect in swarm flight, simulations were carried out with a different number of UAVs based on the quadrotor nonlinear dynamic model. Compared with the classical control method, the simulations demonstrate the superiority in control accuracy.

1. Introduction

Under the distributed combat scenario of the UAVs (unmanned aerial vehicle) swarm, many different types, inexpensive and small-scale UAVs to replace the integrated, large and expensive platforms. The functions of the large platform are decentralized to different small platforms, and achieving different missions can be achieved by combining different types of UAVs with different equipments. Some specific applications such as aerial refueling, close-range data exchange, and collaborative mission execution require two aircrafts to maintain a relatively fixed distance. In addition, the formation of two aircrafts is also a very effective air combat mode formed after a long period of air combat and training practices (Shaw, 1988).

Pairwise flight is standard behavior in natural bird flocks, as shown in Fig. 1. In many bird species, couples often fly together nearby while keeping the whole flock together, forming an exciting phenomenon of small pairwise structures within a large flock structure. In recent years, scientists have collected a large amount of observed data on the flight of the jackdaw swarm (Kings, 2018; Ling et al., 2019c,b,a) and found that the jackdaw swarm contains pairwise sub-structures. The pairwise jackdaws always keep a close distance through the spring-like interaction force (Kings, 2018; Emery et al., 2007; Kubitz et al., 2015; Valletta et al., 2017; Röell, 2008). Through further analysis of how jackdaws flap wings, it can be found that pairwise jackdaws flap wings more slowly than un-pairwise ones in the swarm, which will help save energy (Ling et al., 2019a). In addition, the computer simulations showed that the pairwise structure has a more vital ability to cope

with external environment changes, and the inter-communication load could be reduced significantly (Zhang et al., 2020). However, there are few types of research on how to realize the pairwise control similar to jackdaws.

The current research on UAVs swarm control is based mainly on the assumption that all individuals follow the same interaction rules or control protocols and seldom consider the need for substructures in the swarm. In the aspect of mathematical models, such as Reynolds (1987) proposed the Boid model, summarizing the interaction of bird swarm in flight into three principles: separation, cohesion and alignment. Vicsek et al. (1995) proposed the self-organizing particle model, named the Vicsek model. Olfati-Saber (2006) proposed a flocking control framework. The traditional Olfati-Saber flocking control will form a relatively stable grid structure, which may prevent the pairwise flight in swarm flocking. Firstly, the attraction–repulsion forces among UAVs will prevent the proximity of pairwise UAVs. In the simulation, we found that it is hard to control pairwise UAVs accurately by using the spring-like force of Kings (2018), Emery et al. (2007), Kubitz et al. (2015), Valletta et al. (2017) and Röell (2008). The reasons are: Firstly, the interaction of nearby UAVs will be a very complex disturbance pairwise. Secondly, the attraction–repulsion force is usually nonlinear. Since the UAVs need to maintain a certain distance from each other, a large repulsive force will be produced to avoid collision when the distance is too close. All of these add difficulty to the controller design.

In recent years, sliding mode control has been successfully applied to multi-agent distributed control. Such as Liu et al. (2021) designed

* Corresponding author.

E-mail address: ming_he_2020@126.com (M. He).



Fig. 1. Natural birds flying in pairs (image used with the permission from Dr. Jolle).

a social behavioral-based sliding mode control for the UAVs' swarm motion in multi-UAV air combat. Xiang et al. (2017) adopted full-order sliding mode control for several UAVs flight. Sun et al. (2021) proposed a nonsingular terminal sliding mode control for the mobile robot path tracking control. Ning et al. (2019) proposed a finite time-dependent sliding mode control to control the second-order multi-agent system. Ding et al. (2020) designed a class of novel predefined-time sliding mode surfaces based on the time-regulator function. Yu et al. (2021a) designed a new swarm motion potential function to control the bionic movement for collision avoidance, connectivity preservation, formation generation, and adaptive swarm control (Yu et al., 2021b).

In the traditional sliding mode controller design, the front coefficients $k \text{ sign}(s)$ are usually constant (Utkin et al., 2020), and scholars mainly focus on the chattering caused by the sign function (Singla et al., 2014). Such as Lee and Utkin (2007) used continuous switching functions to replace the sign function. Efimov et al. (2016) introduced a time-delay function to replace the sign function. Li et al. (2022) analyzed the norm-normalized vector sign function deeply.

The main contributions of this article can be summarized as follows.

- (1) We put forward a new pairwise control mode in UAVs flocking to perform short-range cooperative missions of two specific UAVs.
- (2) To realize the relative distance control between UAVs, we propose a new sliding mode control architecture. The significant innovations contain "Quadratic Error Sliding Surface" (QESS) and "Sliding Mode Sign Multiplier" (SMSM). With QESS, we control the system to converge to the specified equilibrium circle. Using SMSM further, we can control all the stable equilibrium points on the circle to converge to 2 or 4 specific stable points, and the system trajectory will slide along the equilibrium circle to converge to the specified angular position. We propose four types of SMSM and show their different control effects in a table. In pairwise distance control, the QESS and the SMSM are used to control two UAVs in the swarm to overcome the disturbance and converge to the specified relative distance.
- (3) To validate the effectiveness and practicability of the proposed methods, we carry out simulations with different numbers of UAVs and the quadrotor nonlinear dynamic model.

The structure of this paper is organized as follows. Section 2 establishes the second-order dynamic model of the swarm. Section 3 proposes a swarm flocking and pairwise control protocol with leaders. Section 4 focuses on designing a sliding mode controller for pairwise control, including the error model, sliding surface design, and corresponding sliding mode controller. Section 5 is the theoretical proof, and it proves the convergence of sliding surface, the convergence of pairwise UAVs distance and the stability of the whole swarm. Section 6 is the computer simulation, where the pairwise number is from 2 (1 pair) to 10 (5 pairs) to analyze and verify the control effect.

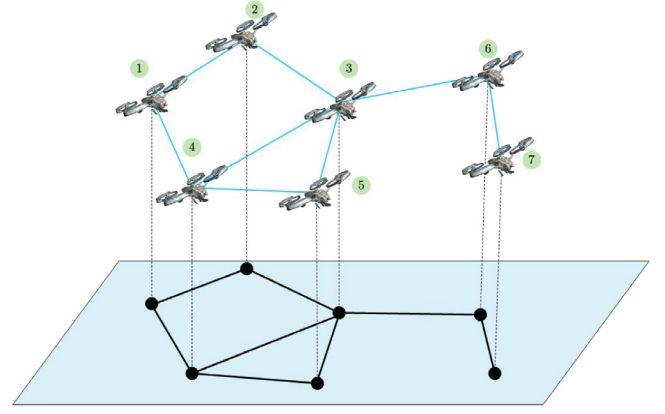


Fig. 2. Graph model of UAVs swarm.

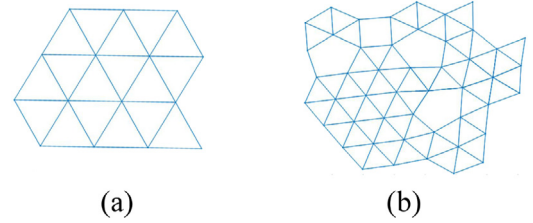


Fig. 3. (a) α -lattices system, (b) α -lattices-like system.

2. Dynamics model of UAVs swarm

Considering that N agents work in n dimensional Euclidean spaces, their dynamics equations can be written as:

$$\begin{cases} \dot{q}_i(t) = p_i(t) \\ \dot{p}_i(t) = u_i(t) \end{cases} \quad i = 1 \dots N \quad (1)$$

where $q_i(t), p_i(t), u_i(t) \in \mathbb{R}^n$ are the position vector, velocity vector and acceleration vector of agent i , and $t \in [0, +\infty)$ (Liu et al., 2018).

An undirected graph $G(t)$ composed of UAVs swarm as shown in Fig. 2. The $G(t)$ consists of nodes and edges of agents at time t , where the set of nodes is represented by $V = \{1, \dots, N\}$. Let $r > 0$ be the perceived radius of the agents, $\|\cdot\|_2$ is the l^2 norm, so that the neighborhood of agent i at time t is defined as:

$$\mathcal{N}_i(t) = \left\{ j \in V \mid j \neq i, \quad \|q_i(t) - q_j(t)\|_2 < r \right\}. \quad (2)$$

The set of edges at the time t is represented by $E(t) = \{(i, j) \in V \times V \mid j \in \mathcal{N}_i(t)\}$.

In order to avoid collision between agents, the agents need to keep a distance more significant than the safe distance r_s while no more than the perceived radius r , so the expected distance of a multi-agent system is defined as:

$$\|q_i(t) - q_j(t)\|_2 = d, (i, j) \in E(t), r_s < d < r. \quad (3)$$

However, due to the interaction of attraction and repulsion between agents, it may be difficult to reach the ideal α -lattices system (Olfati-Saber, 2006) and eventually evolve into α -lattices-like system with error δ as shown in Fig. 3

$$-\delta + d \leq \|q_i(t) - q_j(t)\|_2 \leq \delta + d, (i, j) \in E(t). \quad (4)$$

An externally controllable virtual leader is added (Olfati-Saber, 2006) to guide the UAVs swarm moving in the desired direction. The UAVs in the swarm that can directly receive information from the virtual leader are called pinning nodes (Olfati-Saber, 2006).

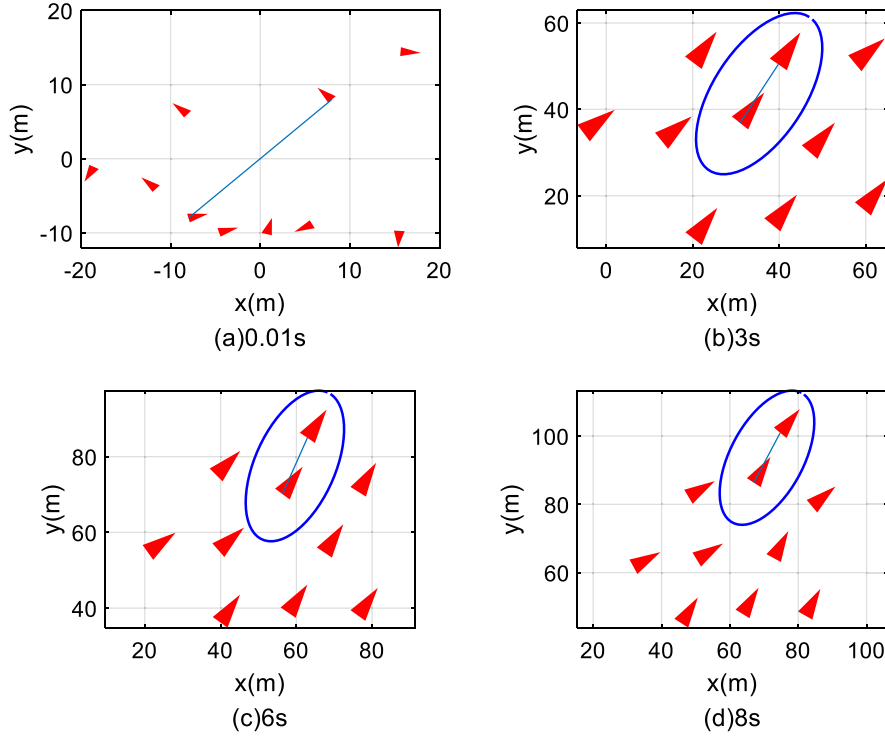


Fig. 4. The positions and directions at different times of 10 UAVs with 1 pair of pairwise UAVs.

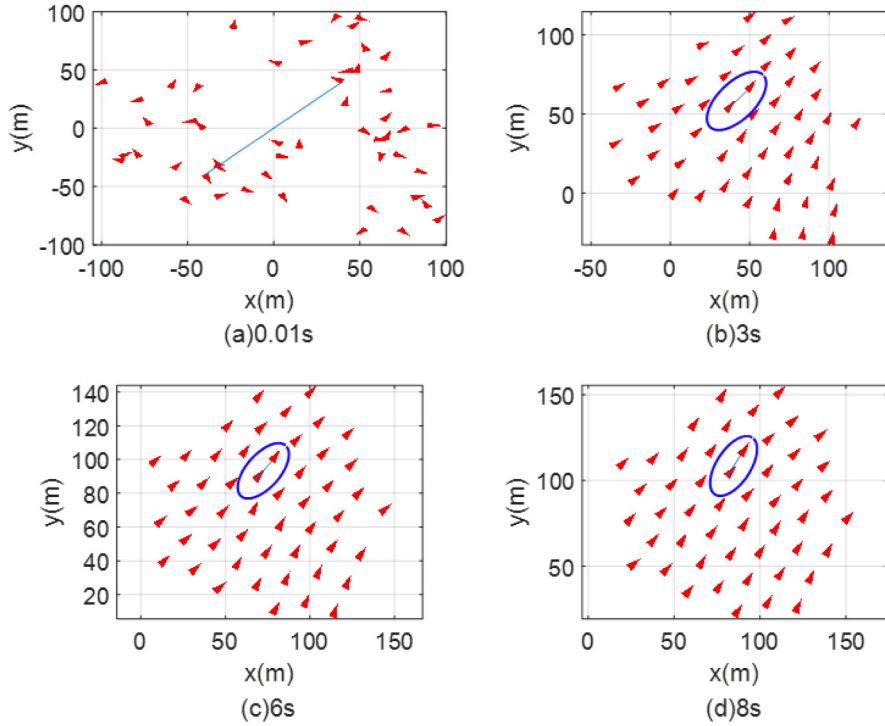


Fig. 5. The positions and directions at different times of 50 UAVs with 1 pair of pairwise UAVs.

Define the mathematical expression h_i as

$$h_i(t) = \begin{cases} 1, & \text{node } i \text{ is pinning node} \\ 0, & \text{node } i \text{ is NOT pinning node} \end{cases} \quad (5)$$

Let the pairwise factor between two different UAVs i and j as h_{ij}^x . The mathematical expression is

$$h_{ij}^x = \begin{cases} 1, & i, j \text{ are pairwise nodes} \\ 0, & i, j \text{ are NOT pairwise nodes} \end{cases} \quad (6)$$

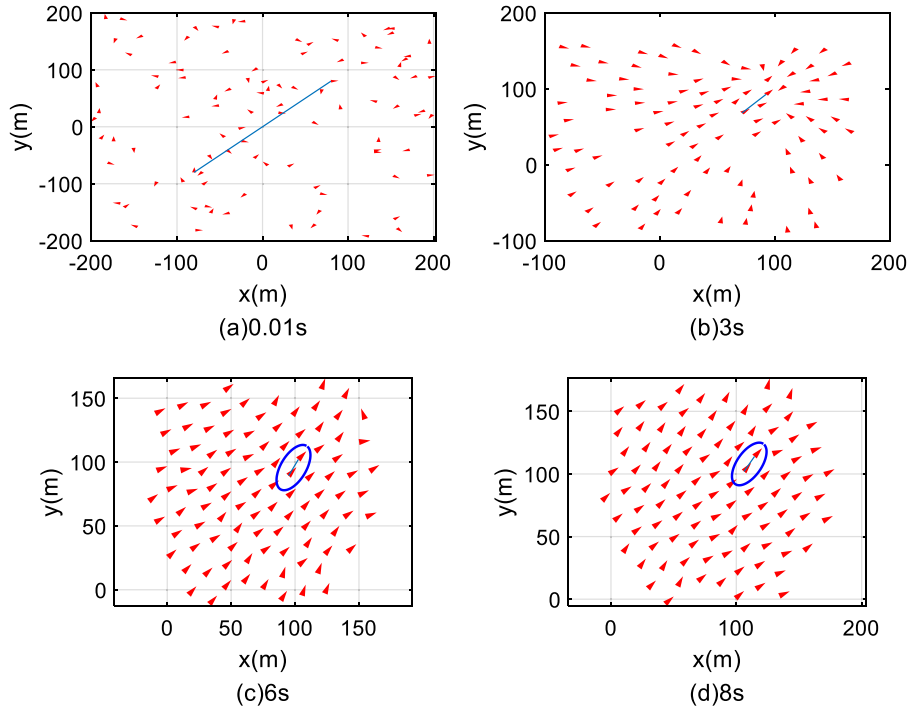


Fig. 6. The positions and directions at different times of 100 UAVs with 1 pair of pairwise UAVs.

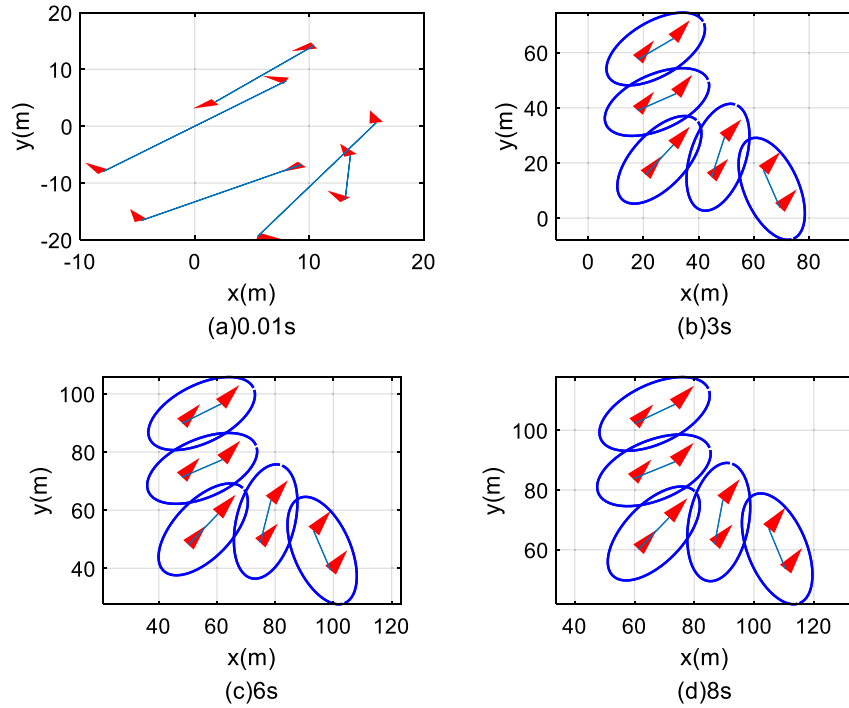


Fig. 7. The positions and directions at different times of 10 UAVs with 5 pairs of pairwise UAVs.

Set $h_{ii}^x = 0$.

The number of pairwise individual UAV i , h_i^x is

$$h_i^x = \sum_{j=1}^N h_{ij}^x. \quad (7)$$

Since each UAV in this paper has one UAV to pair, so $h_i^x = h_j^x = h_{ij}^x = h_{ji}^x$. Nevertheless, the mathematics model can also be extended to more numbers of UAVs to pair in the future.

3. Control protocol of swarm flocking

The control protocol of each UAV $u_i(t)$ is designed to achieve the following goals:

- (a) Distance between neighboring UAVs satisfies formula (4).
- (b) The velocity directions of neighboring UAVs remain aligned.
- (c) All UAVs follow the virtual leader.

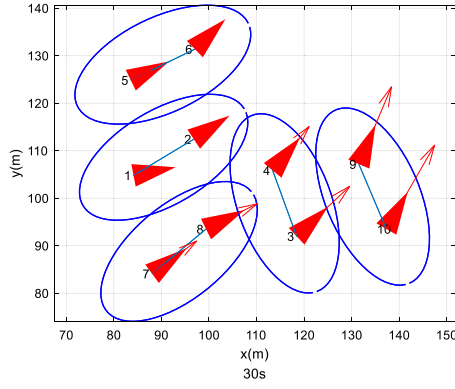


Fig. 8. The positions and directions at the 30 s of 10 UAVs with 5 pairs of pairwise UAVs.

- (d) Distance between the pairwise UAVs A and B is equal to an expected value d_m ,

$$\|q_B(t) - q_A(t)\|_2 = d_m. \quad (8)$$

$u_i(t)$ is the control input of each UAV at time t , which can be defined as

$$u_i(t) = f_i^g(t) + f_i^v(t) + h_i f_i^y(t) + h_i^x f_i^x(t). \quad (9)$$

For brevity, the (t) of $q_i(t), p_i(t), u_i(t), f_i(t)$ is omitted in the following formula. f_i^g is the relative distance control term, which is used for the separation or aggregation. f_i^v is direction consistency control term, which is used for direction alignment. f_i^y is the pinning feedback term used for the pinning nodes to follow the virtual leader. f_i^x is the proposed pairwise control. h_i is the pinning node option term of the virtual leader. h_i^x is the pairwise option term.

A regular distance should be kept between neighboring UAVs when flocking. A continuous attraction–repulsion function is designed in Olfati-Saber (2006). Although the mathematical property is differentiable, the form is too complicated to implement. The distance control in this paper adopts the potential energy function in Gazi and Passino (2004) to analyze and calculate conveniently. The expression of function is

$$f_i^g = \sum_{j \in \mathcal{N}_i} g(q_j - q_i), \quad (10)$$

where $g: \mathbb{R}^n \rightarrow \mathbb{R}^n$ is a function which represents the attraction and repulsion force between different individuals (Gazi and Passino, 2004).

$$g(x) = x [g_a(\|x\|_2) - g_r(\|x\|_2)], \quad (11)$$

Let g_a and g_r satisfy formula Eqn (12), (13) and (14):

$$\begin{cases} g_a(\|e\|_2) > g_r(\|e\|_2), & \text{when } \|e\|_2 > d \\ g_a(\|e\|_2) = g_r(\|e\|_2), & \text{when } \|e\|_2 = d \\ g_a(\|e\|_2) < g_r(\|e\|_2), & \text{when } \|e\|_2 < d \end{cases} \quad (12)$$

$$g_a(\|x\|_2) = a \|x\|_2, \quad (13)$$

$$g_r(\|x\|_2) \|x\|_2 < A_b, \quad (14)$$

where a is control parameter A_b is the upper bound of the system control output.

The speed consistency control term f_i^v is

$$f_i^v = \sum_{j \in \mathcal{N}_i} a_{ij} (p_j - p_i) \quad (15)$$

The pinning feedback term f_i^y is

$$f_i^y(t) = c_1^y (q_y(t) - q_i(t)) + c_2^y (p_y(t) - p_i(t)), \quad (16)$$

where $q_y(t), p_y(t) \in \mathbb{R}^n$ are the position and velocity vector of the virtual leader at the time t , and c_1^y, c_2^y are two regulation parameters.

In general, the following assumptions about the initial conditions of the swarm are made:

Assumption 1. The initial state of the UAVs swarm is connected, which means the initial state $G(0)$ of the undirected graph is connected.

Assumption 2. There is no collision in the initial state of the UAV swarm.

Assumption 3. $h_A = h_B$. The UAVs A and B receive the exact instructions from the virtual leader simultaneously.

Assumption 4. $\text{num}(\mathcal{N}_A(t)) = \text{num}(\mathcal{N}_B(t))$. UAV A has the same neighbor number as B .

4. Design of the pairwise convergent sliding mode controller

The sliding mode control has the advantages of fast response, strong robustness, simple and the precise system parameters are not required (Utkin, 1977). Variable structure sliding mode control is adopted in this paper to achieve precise distance control between pairwise UAVs.

The basic idea of variable structure sliding mode control is to divide the system's motion into two parts. The first part is the motion stage from the initial state to the switching surface, called the arrival stage. The second part is the motion stage of the system on the switching surface, that is, the sliding mode stage. The design of the sliding mode controller could also be divided into two parts. The first part is the sliding surface design, and the second is the design of switching control so that the system state could enter the sliding surface designed in the first part under any initial conditions (Young et al., 1999).

According to the above work, the next step is to establish the system model and design the sliding surface and sliding mode controller.

4.1. Mathematics model of pairwise motion

For pairwise UAVs A and B , another important control goal is to make the distance between A and B converge to an expected value:

$$\begin{cases} \|q_B - q_A\|_2 \rightarrow d_m \\ \|p_B - p_A\|_2 \rightarrow 0 \end{cases} \quad (17)$$

Define pairwise distance state y as

$$y(t) = q_B(t) - q_A(t). \quad (18)$$

For brevity, the (t) is omitted. From (1) and (9), it is easy to get

$$\begin{cases} y = q_B - q_A \\ \dot{y} = p_B - p_A \\ \ddot{y} = u_B - u_A \end{cases} \quad (19)$$

Since $h_B^x = h_A^x = 1$ according to (9) and (19)

$$\ddot{y} = (f_B^g - f_A^g) + (f_B^v - f_A^v) + (h_B f_B^y - h_A f_A^y) + (f_B^x - f_A^x). \quad (20)$$

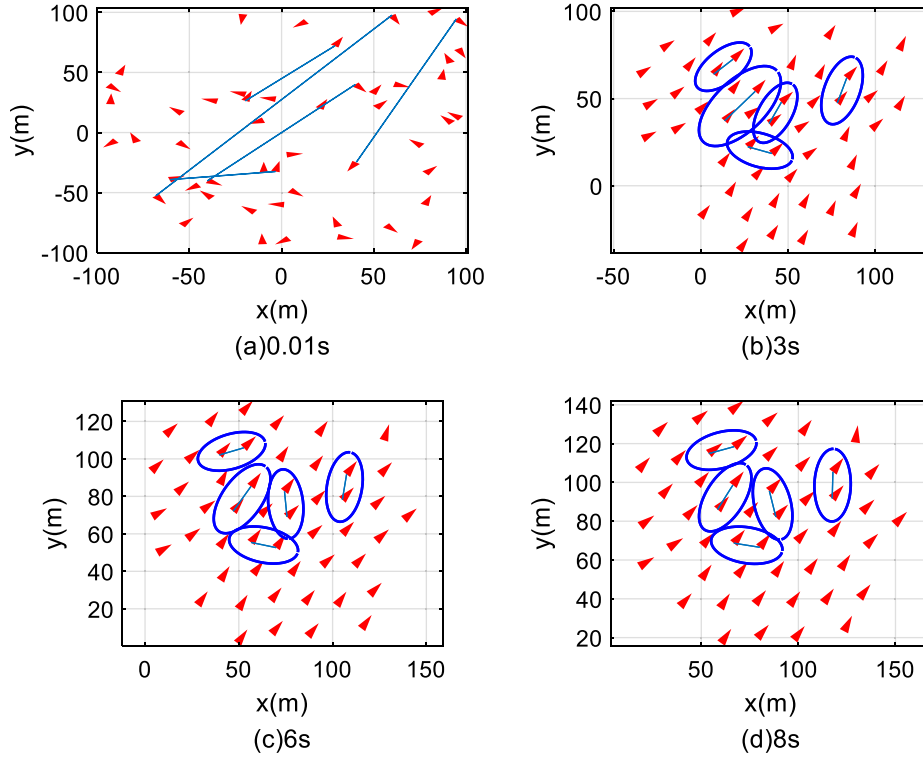


Fig. 9. The positions and directions at different times of 50 UAVs with 5 pairs of pairwise UAVs.

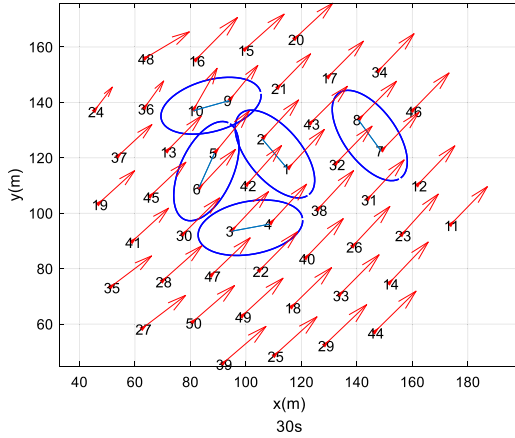


Fig. 10. The positions and directions at the 30 s of 50 UAVs with 5 pairs of pairwise UAVs.

4.2. Design of sliding surface

The error model is modified accordingly to achieve the formula's control goal (17). New tracking error e and sliding surface s are designed as follows:

$$e = (\|y\|_2)^2 - d_m^2 = y^T y - d_m^2, \quad (21)$$

$$\dot{e} = 2y^T \dot{y}, \quad (22)$$

$$s = ce + \dot{e} = cy^T y - cd_m^2 + 2y^T \dot{y} = y^T (cy + 2\dot{y}) - cd_m^2. \quad (23)$$

The quadratic form is used in the sliding surface in (21), making the control target dependent only on the absolute distance but independent of the relative position. Another form is $\|y\|_2 - d_m$. Both control objectives are equivalent, but the differential forms are different. In

contrast, the sliding surface (20) is differentiable everywhere, with better mathematical properties. Another advantage is that the quadratic form only needs to measure the relative distance information between pairwise UAVs and does not need relative direction and angle information. Utilizing TOF (time of flight) or other measurement methods, less communication cost and lower computational complexity are needed, reducing the difficulty of engineering implementation.

4.3. Design of controller

The corresponding reaching law \dot{s} and controller u are designed to make the system move according to the predetermined state track of "sliding mode".

Let $V = \dot{y}^T y$, $E = y^T y$, and the reaching law is designed as follows:

$$\dot{s} = k \text{sign}(s). \quad (24)$$

Based on the design of a nonsingular quadratic error sliding surface, we propose a new sliding mode controller structure by multiplying a new sign function λ on the traditional sign function to change the dynamic characteristics of the control system. Let us name λ as Sliding Mode Sign Multipliers (SMSM). By the SMSM, the system can converge to the specified circle and further slide along the circle to the specified angular position.

The algorithm of SMSM pairwise distance controller is designed as

$$f^x = g(y, \dot{y}) - k\lambda(y)\text{sign}(s), \quad (25)$$

where k is a positive proportional coefficient. In this paper, we select the No.3 SMSM of Table 1, so

$$\lambda(y) = \begin{bmatrix} \text{sign}(y_1 / \|y\|_2) \\ \text{sign}(y_2 / \|y\|_2) \end{bmatrix}. \quad (26)$$

$g(y, \dot{y})$ is the compensation term used to compensate for the system dynamic and the interaction with neighboring UAVs,

$$g(y, \dot{y}) = \frac{1}{2} \left(aNy + bN\dot{y} - c\dot{y} - \frac{V}{E}y \right). \quad (27)$$

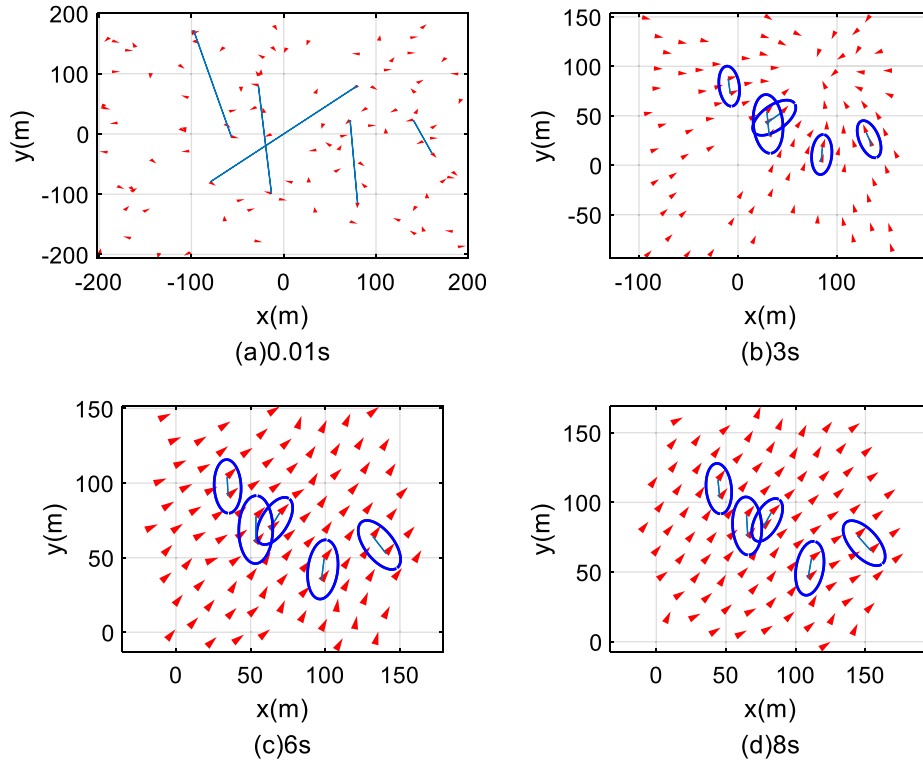


Fig. 11. The positions and directions at different times of 50 UAVs with 5 pairs of pairwise UAVs.

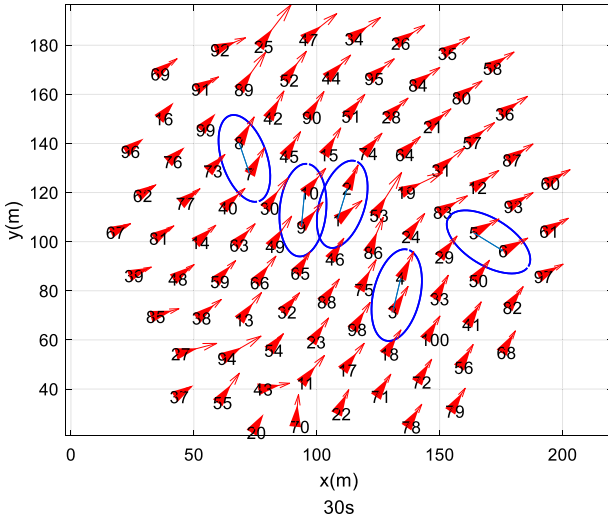


Fig. 12. The positions and directions at the 30 s of 100 UAVs with 5 pairs of pairwise UAVs.

To facilitate graphical display, we analyze the two-dimensional case.

Let $\text{sign}(\mathbf{y}) = \begin{bmatrix} \text{sign}(y_1) \\ \text{sign}(y_2) \end{bmatrix}$, and then $\mathbf{f}_A^x = -\mathbf{f}_B^x = \mathbf{f}^x$.

We propose four types of SMSM and show their formulas and different control effects in Table 1.

5. Theoretical results

In this section, Lyapunov's second method is mainly used to prove the stability of the pairwise control and the swarm system. The proof of sliding mode control is given, and the following Theorems 1 and 2 are proved. On this basis, Theorem 3 is proved. Finally, Theorem 4 is proved that the entire swarm will get into a flocking state.

(Theorem 1) The system converges to $\|\mathbf{y}\|_2 \rightarrow d_m$ when arriving at sliding surface $s = 0$.

(Theorem 2) The variable structure control law \mathbf{u} makes the moving point converge to the switching surface $s = 0$.

(Theorem 3) The distance between pairwise UAVs converges to an expected value.

(Theorem 4) The UAV's swarm will get into a flocking state without collision.

The mathematical statements and proofs of the theorems are as follows.

Theorem 1. If $\mathbf{y}(0) \neq 0$, the dynamics (26) tend to be stable, namely, if $t \rightarrow \infty$, then $e \rightarrow 0$ and $\|\mathbf{y}\|_2 \rightarrow d_m$.

Proof. If $s = 0$ we have

$$\mathbf{y}^T (c\mathbf{y} + 2\dot{\mathbf{y}}) - cd_m^2 = 0, \quad (28)$$

From (28) the first-order nonlinear differential system is

$$\mathbf{y}^T \dot{\mathbf{y}} = \frac{c}{2} d_m^2 - \frac{c}{2} \mathbf{y}^T \mathbf{y}. \quad (29)$$

If $\dot{e} = 0$, a set of stationary solutions of (29) is $\mathbf{y}_s \in \Omega := \{\mathbf{y} : \|\mathbf{y}\|_2 = d_m\}$.

Then let us consider the stability behavior of the stationary solutions.

If $\|\mathbf{y}\|_2 < d_m$, $\mathbf{y}^T \dot{\mathbf{y}} = \frac{c}{2} d_m^2 - \frac{c}{2} \mathbf{y}^T \mathbf{y} > 0 \Rightarrow \nabla \|\mathbf{y}\|_2 = 2\mathbf{y}^T \dot{\mathbf{y}} > 0$.

Similarly, if $\|\mathbf{y}\|_2 > d_m$, $\mathbf{y}^T \dot{\mathbf{y}} = \frac{c}{2} d_m^2 - \frac{c}{2} \mathbf{y}^T \mathbf{y} < 0 \Rightarrow \nabla \|\mathbf{y}\|_2 = 2\mathbf{y}^T \dot{\mathbf{y}} < 0$. Thus, the stability of the stationary solutions is proved.

So, if $t \rightarrow \infty$, $\|\mathbf{y}\|_2 \rightarrow d_m$, which means it finally converges to the sphere $\mathbf{y}_s \in \Omega := \{\mathbf{y} : \|\mathbf{y}\|_2 = d_m\}$.

Theorem 2. The sliding surface shown in (23) the pairwise controller (25), the moving point converges to the switching surface $s = 0$ in a limited time under the control of (9).

Proof. Lyapunov function is designed as follows:

$$V = \frac{1}{2} s^2. \quad (30)$$

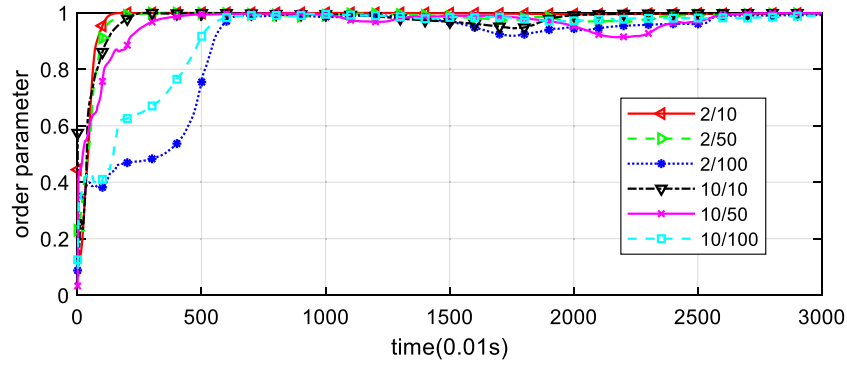


Fig. 13. Velocity direction order parameter (pairwise UAVs/total UAVs).

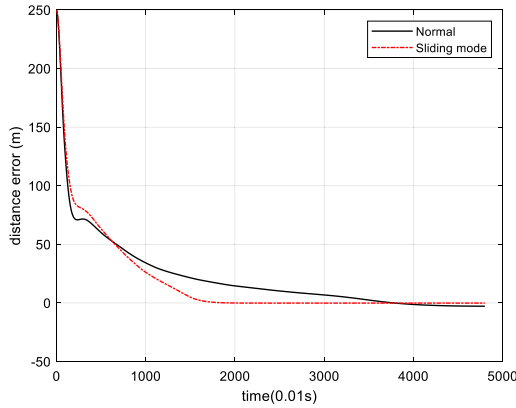


Fig. 14. The comparison of distance errors between the classical method and sliding mode method.

After the derivation of the designed Lyapunov function, the controller (9) is substituted

$$\begin{aligned} \dot{s} &= 2cy^T \dot{y} + 2\dot{y}^T \dot{y} + 2y^T \ddot{y} \\ &= 2cy^T \dot{y} + 2\dot{y}^T \dot{y} + 2y^T (-aN\dot{y} - bN\ddot{y} + f_{mn}^T + 2f^T) \\ &= 2y^T (-aN\dot{y} + (c - bN)\ddot{y}) + 2\dot{y}^T \dot{y} + 2y^T (f_{mn}^T + 2f^T) \\ &= 2y^T (-ksign(s)sign(y) + 2f_{mn}^T) \end{aligned} \quad (31)$$

$$\dot{V} = \dot{s}s = 2y^T (-ksign(s)\lambda(y) + 2f_{mn}^T)s, \quad (32)$$

where $f_{mn}^T = f_n^T - f_m^T$. Since the repulsion force is bounded $\|f_{mn}^T\|_\infty < \delta$ and δ is an upper bound. In this case, we select the No.3 SMSM of Table 1, so we have $y^T \lambda(y) \geq 0$.

If $k > 2\delta$ $\dot{V} = \dot{s}s < 0$ and the sliding surface is reachable.

If $\dot{V} \equiv 0$, $s \equiv 0$. According to the LaSalle invariance principle, the closed-loop system is stable. When $t \rightarrow \infty$, $s \rightarrow 0$. Thus, the Theorem 2 is proved.

From Theorems 1 and 2, the following theorems can be obtained:

Theorem 3. For the two UAVs in the swarm that need to be pairwise, the sliding surface (23) and the pairwise controller (25). The distance between pairwise UAVs converges to the expected value.

Proof. From the result of Theorem 2, when $t \rightarrow \infty$, $s \rightarrow 0$.

When $s = 0$, $s = ce + \dot{e} = 0 \Rightarrow e(t) = e(0)\exp(-ct)$, where $\exp()$ is the exponential function, we use it to avoid confusion with the tracking error symbol e .

So, when $t \rightarrow \infty$, $e = ((\|y\|_2)^2 - d_m^2) \rightarrow 0$. Thus, the Theorem 3 is proved.

Theorem 4. In the UAVs swarm system, the UAV motion equation is shown as formula (1), and the control protocol is shown as formula (9). For any single or multiple UAVs are chosen as the pinning nodes, the conclusions can be obtained:

- (1) The relative positions of all UAVs will eventually tend to lattices.
- (2) The speed of all UAVs will tend to the speed of the virtual leader $p_\gamma(t)$.
- (3) There will be no collision among the UAVs swarm.
- (4) The positions of the pinning nodes will tend to the position of the virtual leader $q_\gamma(t)$.

Proof. Suppose the tracking error between UAVs and the virtual leader is:

$$\tilde{q}_i(t) = q_i(t) - q_\gamma(t), \tilde{p}_i(t) = p_i(t) - p_\gamma(t), \quad (33)$$

Suppose the distance between UAVs is:

$$q_{ij}(t) = q_i(t) - q_j(t), \quad (34)$$

Then

$$q_{ij}(t) = \tilde{q}_i(t) - \tilde{q}_j(t). \quad (35)$$

The potential energy function of a single UAV is

$$U_i(t) = \sum_{j=1, j \neq i}^N \Phi_i(q_{ij}) + \frac{1}{2} h_i c_1 \tilde{q}_i^T \tilde{q}_i, \quad (36)$$

where

$$\Phi_i(q_{ij}) = \frac{1}{2} \sum_{j \in N_i(t)} ((q_{ij}(t))^T q_{ij}(t) - d^2), \quad (37)$$

If there is no overlap among UAVs, $q_i \neq q_j$. that is, $\tilde{q}_i(t) \neq \tilde{q}_j(t)$. When using the attraction and repulsion functions of formula (10), there is

$$\nabla_x \Phi(\|x\|_2) = xg(\|x\|_2) \quad (38)$$

If $\|x\|_2 = d$, the value Φ is minimum.

Let the total system energy of the UAVs swarm be $Q(t)$, including the total kinetic energy and potential energy of all UAVs are expressed as follows:

$$Q(t) = \frac{1}{2} \sum_{i=1}^N (U_i(t) + \tilde{p}_i(t)^T \tilde{p}_i(t)). \quad (39)$$

The difference between the controller compared with (Olfati-Saber, 2006) mainly lies in the gradient-based term. To prove the stability of our flocking model, using the same technique as described in the STABILITY ANALYSIS OF FLOCKING of Olfati-Saber (2006), we can obtain $\dot{Q} < 0$ that the system's total energy will decay continuously.

$$Q(t) < Q_0 < Q_{\max}. \quad (40)$$

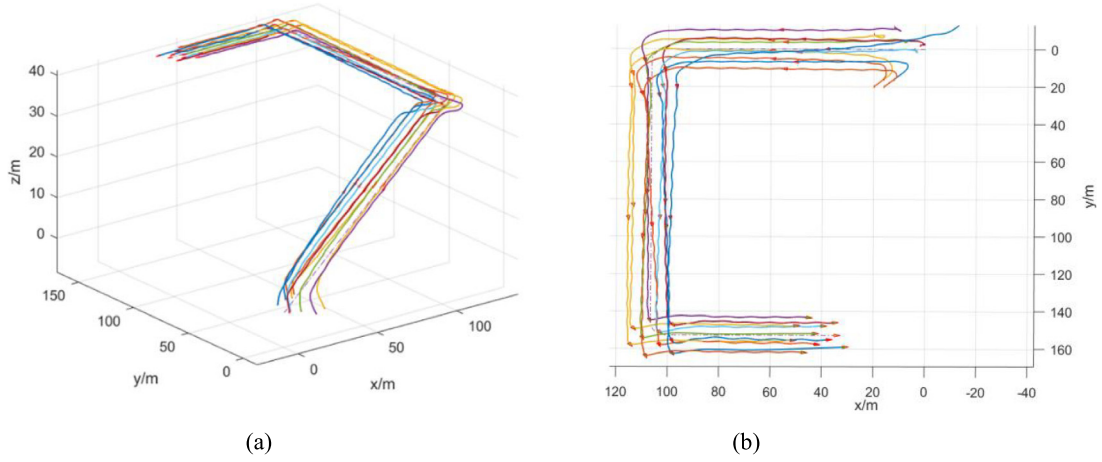


Fig. 15. The trajectory of UAVs swarm.

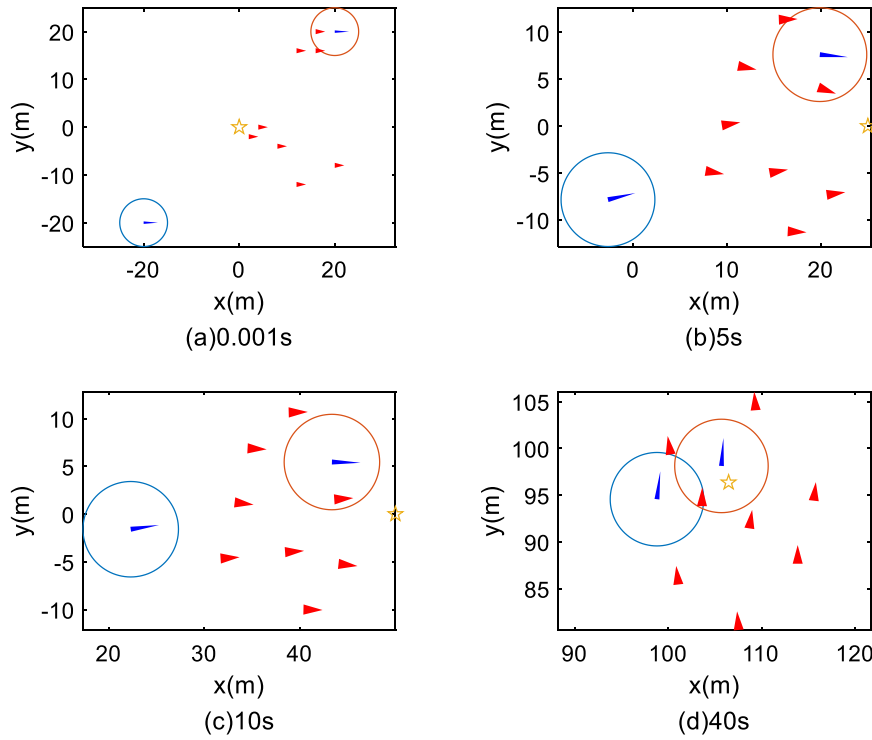


Fig. 16. Positions of UAVs at different time.

According to the definition of the potential energy function $U(q)$, $\sum_{i=1}^N U_i(\|r\|_\alpha) < Q(0) < Q_{\max}$. However, the distance between two neighboring nodes at time t should be less than r , so the existing edge in the network will not break. Suppose that after Δt time, M edges are added to the network. Then

$$Q(t + \Delta t) = Q_0 + mU(\|r - \varepsilon\|_\alpha) < Q_{\max}. \quad (41)$$

This indicates that the existing edges in the system will not break over time. The initial network $G(0)$ is connected, so the system will always remain connected.

In general, suppose that $[t_0, t_1]$ a UAV i j collided at $t_s \in [t_0, t_1]$. Then $\Phi_i(t)$ it will increase, and the total energy $Q(t)$ will increase, which is contradicted with $\dot{Q}(t) \leq 0$. Therefore, the UAVs will not collide. Similarly, the UAVs swarm will not collide during each period $[t_k, t_{k+1}]$.

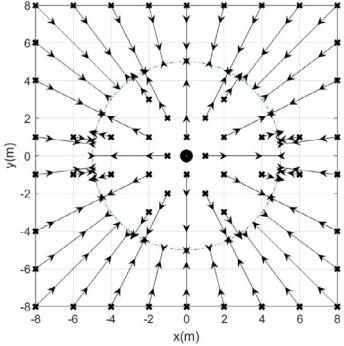
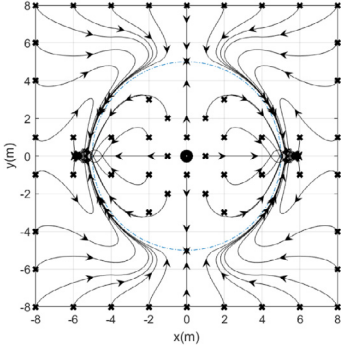
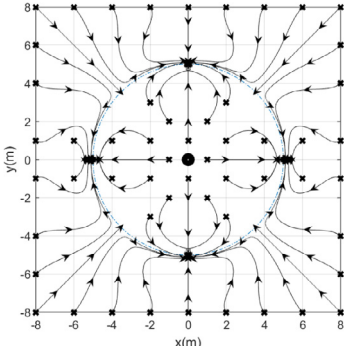
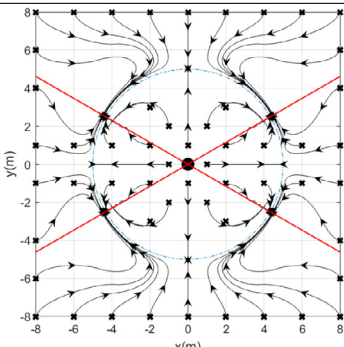
In addition, from Su et al. (2009), the theorem is proved.

6. Simulation

To verify the influence of pairwise UAVs on flocking flight, 6 groups of simulations were carried out under the number scale of $N = 10$, $N = 50$, $N = 100$ and the numbers of pairwise UAVs are 1 pair and 5 pairs respectively. The influence of pairwise on direction consistency pairing on cluster is compared and analyzed. Compared with R. Olfati-Saber's classical control method (Olfati-Saber, 2006), the advantage of control accuracy is verified. Finally, based on the quadrotor six freedom-degree nonlinear dynamic models (MathWorks, 2022a,b), the simulation of pairwise UAVs in 10 UAVs swarm is carried out. The flight control system utilized the continuous high-order sliding mode position controller (Liu et al., 2017).

In the simulation, the UAV swarm is set to move in the two-dimensional space plane, and the initial positions of all the UAVs are randomly distributed in $4N \times 4N$ m² area. The expected distance $d_m = 20$ m. The initial position of the virtual leader is (25, 25), and the velocity is constant (0.5, 0.5).

Table 1
Comparison of four types of sliding mode sign multipliers.

No.	Trajectories	Mathematical formula	Notes
1		$\lambda(y) = \begin{bmatrix} 1 \\ 1 \end{bmatrix}$	The starting points can be attracted to the circle O_r by the shortest path, and any point on O_r is the stable equilibrium point.
2		$\lambda(y) = \begin{bmatrix} 1 \\ \text{sign}(y_2 / \ y\ _2) \end{bmatrix}$	The starting points can be attracted to the circle O_r and sliding alone O_r to the stable equilibrium points. The stable equilibrium points are $\theta = 0, \pi$, and the unstable equilibrium points are $\theta = \pm\pi/2$.
3		$\lambda(y) = \begin{bmatrix} \text{sign}(y_1 / \ y\ _2) \\ \text{sign}(y_2 / \ y\ _2) \end{bmatrix}$	The starting points can be attracted to the circle O_r and sliding alone O_r to the stable equilibrium points. The stable equilibrium points are $\theta = 0, \pi, \pm\pi/2$.
4		$\lambda(y) = \begin{bmatrix} \text{sign}(y_1 / \ y\ _2 - \cos(\theta_s)) \\ \text{sign}(y_2 / \ y\ _2 - \sin(\theta_s)) \end{bmatrix}$	The starting points can be attracted to the circle O_r and sliding alone O_r to the stable equilibrium point. The stable equilibrium points are $\theta = \pm\theta_s, \pi \pm \theta_s$. What is shown in the graph is $\theta_s = \pi/6$.

O_r : the circle whose center is at the origin of coordinates and radius is r .

$P(r, \theta)$: The point on the circle O_r $\theta \in (-\pi, \pi]$ is the angle in polar coordinates.

In the drawing, each small triangle represents a UAV, and the acute angle of the triangle indicates the direction of the UAV. The UAVs connected by solid lines indicate the UAVs that need to be pairwise. The pairwise UAVs are enclosed by an ellipse when they have reached the pairwise distance.

6.1. UAVs swarm simulation contains one pair

Firstly, the influence of scale on UAVs swarm to pairwise is verified. The four subgraphs of Figs. 4, 5, and 6 respectively show UAVs' positions and directions at different times when the scales of UAVs

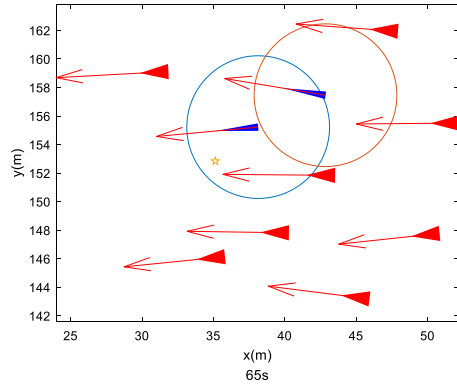


Fig. 17. Positions of UAVs at the final time.

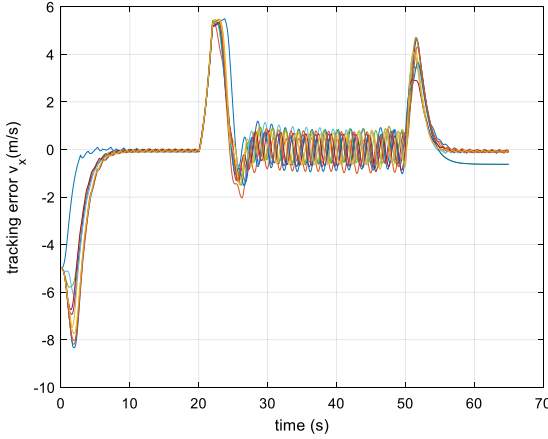


Fig. 18. The velocity errors in the x-axis between UAVs and virtual leader.

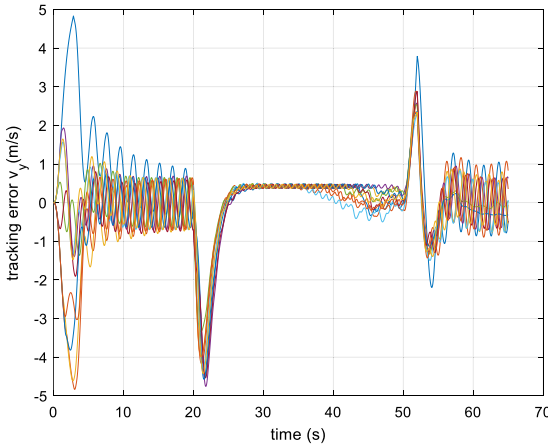


Fig. 19. The velocity errors in the y axis between UAVs and virtual leader.

are 10, 50, and 100. The distances between pairwise UAVs gradually approached over time, which verified the correctness of Theorem 3. At the same time, the speeds of all UAVs tended to be the same and approached the speed of virtual leaders gradually, which verified the correctness of Theorem 4.

6.2. UAVs swarm simulation contains 5 pairs

To verify the flight effects furtherly when the pairwise UAVs are increased to 5 pairs. The four subplots of Figs. 7, 9 and 11 showed the

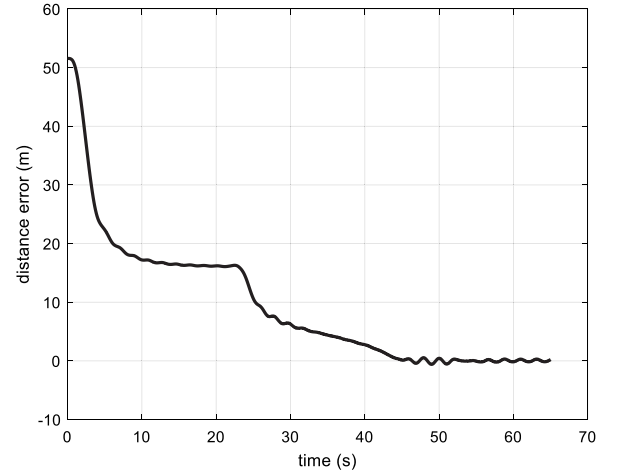


Fig. 20. Distance error between pairwise UAVs.

positions and movements of UAVs at different times when the scales of UAVs are 10, 50 and 100, respectively. Figs. 8, 10 and 12 showed the UAVs' positions and velocities at the end of the 30 s simulation time. The distances between the pairwise UAVs gradually converged with time, while the velocities of all the UAVs tended to be the same and gradually converged to the velocity of the virtual leader.

6.3. Velocity direction order parameter

The influence of pairing on swarm direction consistency is analyzed by calculating the velocity direction order parameter.

The velocity direction order parameter Φ is defined as

$$\Phi = \left\| \frac{1}{N} \sum_i \frac{\mathbf{v}_i}{\|\mathbf{v}_i\|_2} \right\|_2. \quad (42)$$

Φ describes the degree of order of individual movement, or named velocity consistency. When $\Phi = 0$ all the movement directions of UAVs are random and the swarm is entirely disordered. When $\Phi = 1$ all the movement directions of UAVs are the same and the swarm is ultimately ordered. When $\Phi = 0.9$ the swarm will show apparent order (Cavagna and Giardina, 2014).

The variation of order parameters with time is shown in Figure 13 when “pairwise UAVs/total UAVs” is 2/10, 2/50, 2/100, 10/10, 10/50, 10/100. The UAV swarms can achieve consistency ($\Phi > 0.9$) quickly even if the number and the configurations are different. When the scale of a UAV swarm is more significant than 100, the convergence speed is relatively slow due to the scale of the swarm (see Fig. 13).

6.4. Comparative simulation with the classical control method

The scale of UAVs in the simulation is 100. As a comparison simulation, the pairwise distance control term is replaced with the distance control method proposed in the (Olfati-Saber, 2006). On this basis, the parameter k_m is added to adjust the control pairwise distance more precise. The other control terms remain unchanged, which is named as the classical method.

$$\mathbf{f}_i^{\chi}(t) = -k_m (\mathbf{q}_i(t) - \mathbf{q}_m(t)) \left(1 - k_m d_m \|\mathbf{q}_i(t) - \mathbf{q}_m(t)\|_2^{-2} \right). \quad (43)$$

By a large number of parameters tuning, the fine parameters are $k = 0.6, k_m = 2$. When pairwise UAVs/total UAVs = 2/100, The comparison effect of distance error between classical method and sliding mode method is shown in Fig. 14. The steady-state error of the classical method is 2.5 m, and the steady-state error of the sliding mode method of this paper is 0.1 m.

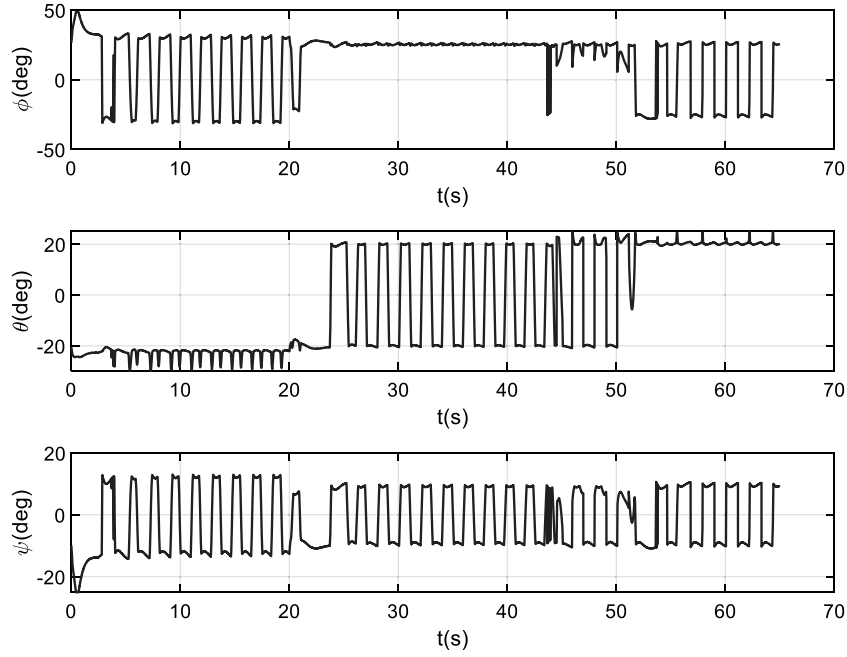


Fig. 21. Euler angle commands output of position controller.

6.5. Flight simulation based on quadrotor UAV dynamics

To further verify the algorithm's effectiveness for the control of quadrotor UAVs, the swarm flight simulations of 10 quadrotor UAVs, including climbing, turning and straight-line flight are carried out based on the dynamics model in Mahony et al. (2012). The quadrotor flight control system utilizes the continuous high-order sliding mode position controller (Liu et al., 2017) and SO(3) attitude controller (Liu et al., 2016). The simulator uses KK-Swarm (KK-Swarm, 2022).

The model parameters of the quadrotor UAV utilize the data of the EMAX UAV provided by the flight measurement website of the Beihang Reliable Flight Control Research Group (Quan, 2022), the mass $mass = 0.6$ kg and the rotational inertia matrix is

$$J = \begin{bmatrix} 3.544 & 0 & 0 \\ 0 & 3.544 & 0 \\ 0 & 0 & 6.935 \end{bmatrix} \times 10^{-3} \text{ kg m}^2. \quad (44)$$

Let the UAV carry out straight-line motion with a speed of 5 m/s—the simulation duration $T = 65$ s. The virtual leader climbs from 0 to 20 s smoothly turns 90° at the moments of 20–22 s, 50–52 s and 70–72 s respectively. Fly in a straight line at other times.

The triangles inside the circle represent the UAVs that needed to be pairwise—the circle's radius $r = d_m$.

The flight path of the Quadrotor UAVs swarm followed by the virtual leader is shown in Fig. 15. (a) is the three-dimensional motion trajectory and (b) is the 2-D motion trajectory. The positions of the UAVs at different times are shown in Fig. 16. The position of the UAV at the final time $T = 65$ s is shown in Fig. 17. The direction of the arrow represents the velocity direction and the length of the arrow indicates the velocity magnitude of the UAV. The triangle inside the circle is the UAV needed to be paired, and the radius of the circle is equal to the expected distance between the two UAVs, which is $r = d_m = 5$ m. The simulation shows that the quadrotor UAV swarm can achieve a satisfied swarming flight and follow the leader.

Figs. 18 and 19 show the velocity components errors on x -axis and y -axis respectively between the UAV and the virtual leader. The tracking error is significant when the virtual leader turns suddenly. However, the final speed of all UAVs is roughly the same as that of the virtual leader.

The distance between the pairwise UAVs converged to d_m and the tracking error is shown in Fig. 20.

Take the No.1 UAV as an example to analyze the attitude tracking response. The output of the position controller is converted into the pull command and the Euler angle command of the attitude controller. The Euler angular commands are shown in Fig. 21. The actual attitude angle of the UAV is shown as Fig. 22. the UAV is able to track the Euler angle command, but there are still existing delays due to the inertia of UAV itself, which causes a slight oscillation during flight. Nevertheless, it does not affect the whole's pairwise control and swarm flight.

7. Conclusion

The pairwise sub-structure control problem in UAVs swarm is put forward in this paper for the first time, which provides a new thought for the cooperative control model of UAVs swarm, especially for the UAVs with a limited load. In the control protocol design, the sliding surface and pairwise sliding mode controller based on quadratic law error are proposed, and the theorems of sliding mode stability and finite-time convergence of moving points to the switching surface of the pairwise control system are proved. Then, the conclusions are proved that sliding mode stability of the pairwise control system and the moving point converge to the switching surface in finite time. The swarming flight of 10, 50 and 100 UAVs was simulated respectively with 1 pair and 5 pairs of pairwise UAVs. To verify the control effect of different UAVs, the pair number of pairwise UAVs was increased from 1 to 5, while the total UAV number was 10, 50 to 100. Furtherly, the swarm flight simulation of 10 UAVs based on the quadrotor UAV dynamic model is used to verify the effectiveness of pairing control. The simulation results show that the effective pairwise control can be achieved for different UAVs numbers, but the system response speed will affect the pairwise accuracy.

The pairwise UAVs will take some special missions based on this paper in the next step. Integrating the pairwise control into a specific UAV dynamics system while realizing accurate and fast pairing needs further research.

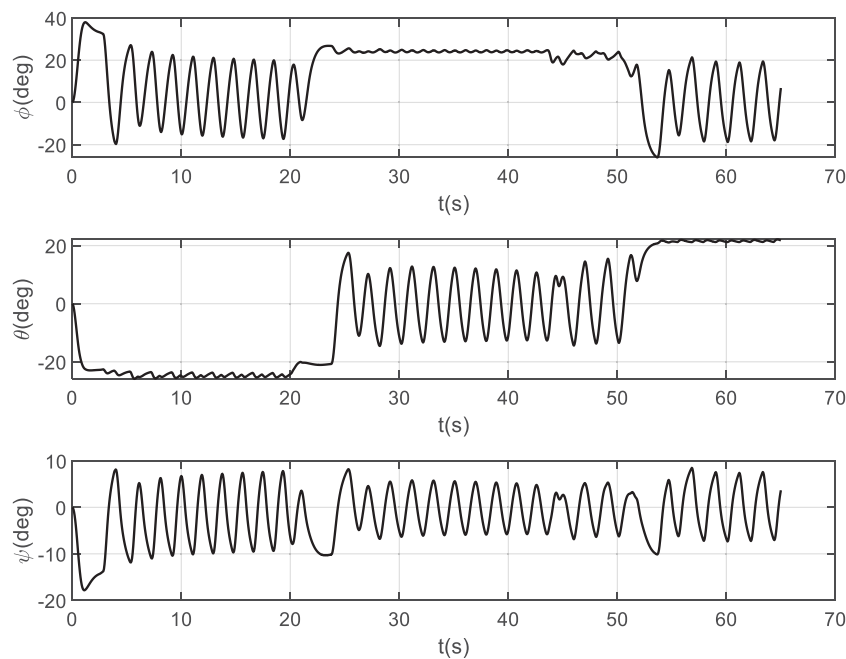


Fig. 22. Euler angles of UAVs.

CRedit authorship contribution statement

Jintao Liu: Conceptualization, Methodology, Software, Writing – original draft. **Ming He:** Supervision, Data curation. **Peng Xu:** Visualization, Investigation. **Xiangyang Deng:** Validation, Writing – reviewing and editing.

Declaration of competing interest

The authors declare that they have no known competing financial interests or personal relationships that could have appeared to influence the work reported in this paper.

Supports

This work was supported by National Postdoctoral Science Foundation of China, No. 2019M663972; Provincial Postdoctoral Science Foundation of Jiangsu, China, No. 2019K185; Provincial Primary Research & Development Plan of Jiangsu, China, No. BE2018754, BE2019762, BE2020729, BE2021729; Military Scientific Research Project, China, No. LJ20212Z010032, LJ20212C011129, LJ20202C020493, Military key research project, China, No. JYKYA2021029.

References

- Cavagna, A., Giardina, I., 2014. Bird flocks as condensed matter. *Annu. Rev. Condens. Matter Phys.* 5 (1), 183–207.
- Ding, T.F., Ge, M.F., Liu, Z.W., Wang, Y.W., Karimi, H.R., 2020. Discrete-communication-based bipartite tracking of networked robotic systems via hierarchical hybrid control. *IEEE Trans. Circuits Syst. I* 67 (4), 1402–1412.
- Efimov, D., Polyakov, A., Fridman, L., Perruquetti, W., Richard, J.P., 2016. Delayed sliding mode control. *Automatica* 64.
- Emery, N.J., Seed, A.M., Von Bayern, A.M.P., Clayton, N.S., 2007. Cognitive adaptations of social bonding in birds. *Philos. Trans. R. Soc. B* 362 (1480), 489–505.
- Gazi, V., Passino, K.M., 2004. A class of attractions/repulsion functions for stable swarm aggregations. *Internat. J. Control* 77 (18), 1567–1579.
- Kings, M., 2018. Foraging Tactics and Social Networks in Wild Jackdaws. University of Exeter.
- KK-Swarm, 2022, KK, KK robot swarm. <https://github.com/kkswarm/kk-robot-swarm>.

- Kubitz, R.J., Bugnyar, T., Schwab, C., 2015. Pair bond characteristics and maintenance in free-flying jackdaws *Corvus monedula*: Effects of social context and season. *J. Avian Biol.* 46 (2), 206–215.
- Lee, H., Utkin, V.I., 2007. Chattering suppression methods in sliding mode control systems. *Annu. Rev. Control* 31 (2), 179–188.
- Li, D., Ge, S.S., Lee, T.H., 2022. Simultaneous arrival to origin convergence: Sliding-mode control through the norm-normalized sign function. *IEEE Trans. Automat. Control* 67 (4), 1966–1972.
- Ling, H., McIvor, G.E., van der Vaart, K., Vaughan, R.T., Thornton, A., Ouellette, N.T., 2019a. Costs and benefits of social relationships in the collective motion of bird flocks. *Nat. Ecol. Evol.* 3 (6), 943–948.
- Ling, H., et al., 2019b. Behavioural plasticity and the transition to order in jackdaw flocks. *Nature Commun.* 10 (1), 5174.
- Ling, H., et al., 2019c. Collective turns in jackdaw flocks: Kinematics and information transfer. *J. R. Soc. Interface* 16 (159), 20190450.
- Liu, J.-T., Gao, L., Wu, W.-H., Li, J., 2017. Image-based target tracking control for vertical take-off and landing UAVs. *Kongzhi Lilun Yu Yingyong/Control Theory Appl.* 34 (6).
- Liu, Q., He, M., Xu, D., Ding, N., Wang, Y., 2018. A mechanism for recognizing and suppressing the emergent behavior of UAV swarm. *Math. Probl. Eng.* 2018, 1–14.
- Liu, C., Sun, S., Tao, C., Shou, Y., Xu, B., 2021. Sliding mode control of multi-agent system with application to UAV air combat. *Comput. Electr. Eng.* 96, 107491.
- Liu, J.-T., Wu, W.-H., Li, J., Xin, Q., 2016. Sliding mode variable structure attitude controller design of quadrotor UAVs on SO(3). *Kongzhi Yu Juece/Control Decis.* 31 (6).
- Mahony, R., Kumar, V., Corke, P., 2012. Multirotor aerial vehicles: Modeling, estimation, and control of quadrotor. *Robot. Autom. Mag. IEEE* 19 (3), 20–32.
- MathWorks, 2022a, MathWorks, Quadcopter Project. <https://www.mathworks.com/help/aeroblks/quadcopter-project.html>.
- MathWorks, 2022b, MathWorks, Six Degree of Freedom Motion Platform. <https://www.mathworks.com/help/aeroblks/six-degree-of-freedom-motion-platform.html>.
- Ning, B., Han, Q.L., Zuo, Z., 2019. Practical fixed-time consensus for integrator-type multi-agent systems: A time base generator approach. *Automatica* 105.
- Olfati-Saber, R., 2006. Flocking for multi-agent dynamic systems: Algorithms and theory. *IEEE Trans. Automat. Control* 51 (3), 401–420.
- Quan, Q., 2022. Flight Evaluation. <https://www.flyeval.com/>.
- Reynolds, C.W., 1987. Flocks, herds and schools: A distributed behavioral model. In: *Proceedings of the 14th Annual Conference on Computer Graphics and Interactive Techniques - SIGGRAPH '87*, Vol. 21. no. 4, pp. 25–34.
- Röell, A., 2008. Social behaviour of the jackdaw, *Corvus monedula*, in relation to its niche. *Behaviour* 64 (1–2), 1–122.
- Shaw, R.L., 1988. *Fighter Combat: The Art and Science of Air-to-Air Combat*. Haynes Publishing Group.
- Singla, M., Shieh, L.S., Song, G., Xie, L., Zhang, Y., 2014. A new optimal sliding mode controller design using scalar sign function. *ISA Trans.* 53 (2).
- Su, H., Wang, X., Lin, Z., 2009. Flocking of multi-agents with a virtual leader. *IEEE Trans. Automat. Control* 54 (2), 293–307.

- Sun, Z., Xie, H., Zheng, J., Man, Z., He, D., 2021. Path-following control of Mecanum-wheels omnidirectional mobile robots using nonsingular terminal sliding mode. *Mech. Syst. Signal Process.* 147.
- Utkin, V.I., 1977. Variable structure systems with sliding modes. *IEEE Trans. Automat. Control* 22 (2), 212–222.
- Utkin, V., Poznyak, A., Orlov, Y.V., Polyakov, O., 2020. *Road Map for Sliding Mode Control Design*. Springer Nature, Switzerland AG.
- Valletta, J.J., Torney, C., Kings, M., Thornton, A., Madden, J., 2017. Applications of machine learning in animal behaviour studies. *Anim. Behav.* 124, 203–220.
- Vicsek, T., Czirak, A., Ben-Jacob, E., Cohen, I., Shochet, O., 1995. Novel type of phase transition in a system of self-driven particles. *Phys. Rev. Lett.* 75 (6), 1226–1229.
- Xiang, X., Liu, C., Su, H., Zhang, Q., 2017. On decentralized adaptive full-order sliding mode control of multiple UAVs. *ISA Trans.* 71.
- Young, K.D., Utkin, V.I., Ozguner, U., 1999. A control engineer's guide to sliding mode control. *IEEE Trans. Control Syst. Technol.* 7 (3), 328–342.
- Yu, D., Chen, C.L.P., Xu, H., 2021a. Intelligent decision making and bionic movement control of self-organized swarm. *IEEE Trans. Ind. Electron.* 68 (7).
- Yu, D., Long, J., Chen, C.L.P., Wang, Z., 2021b. Adaptive swarm control within saturated input based on nonlinear coupling degree. *IEEE Trans. Syst. Man Cybern. Syst.*
- Zhang, L., Bin Duan, H., Yong, T., Deng, Y.M., Wei, C., 2020. Unmanned aerial vehicle swarm formation control based on paired interaction mechanism in jackdaws. *J. Beijing Univ. Aeronaut. Astronaut.* 47 (2), 391–397.